J Paleolimnol (2013) 50:519–533
DOI 10.1007/s10933-013-9743-5

ORIGINAL PAPER

A chrysophyte stomatocyst-based reconstruction of cold-season air temperature from Alpine Lake Silvaplana (AD 1500–2003); methods and concepts for quantitative inferences

Rixt de Jong · Christian Kamenik · Karlyn Westover · Martin Grosjean

Received: 17 July 2012 / Accepted: 19 August 2013 / Published online: 4 September 2013

Abstract Relatively little is known about past cold-season temperature variability in high-Alpine regions because of a lack of natural cold-season temperature proxies as well as under-representation of high-altitude sites in meteorological, early-instrumental and documentary data sources. Recent studies have shown that chrysophyte stomatocysts, or simply cysts (sub-fossil algal remains of *Chrysophyceae* and *Synurophyceae*), are among the very few natural proxies that can be used to reconstruct cold-season temperatures. This study presents a quantitative, high-resolution (5-year), cold-season (Oct–May) temperature reconstruction based on sub-fossil chrysophyte stomatocysts in the annually laminated (varved) sediments of high-Alpine Lake Silvaplana, SE Switzerland (1,789 m a.s.l.), since AD 1500. We first explore the method used to translate an ecologically meaningful variable based on a biological proxy into a simple climate variable. A transfer function was applied to reconstruct the 'date of spring mixing' from cyst assemblages. Next, statistical regression models were tested to convert the reconstructed 'dates of spring mixing' into cold-season surface air temperatures with associated errors. The strengths and weaknesses of this approach are thoroughly tested. One much-debated, basic assumption for reconstructions ('stationarity'), which states that only the environmental variable of interest has influenced cyst assemblages and the influence of confounding variables is negligible over time, is addressed in detail. Our inferences show that past cold-season air-temperature fluctuations were substantial and larger than those of other temperature reconstructions for Europe and the Alpine region. Interestingly, in this study, recent cold-season temperatures only just exceed those of previous, multi-decadal warm phases since AD 1500. These findings highlight the importance of local studies to assess natural climate variability at high altitudes.

Keywords Climate change · Golden algae · Winter-spring temperature variability · Varves · Transfer functions · Calibration in time

R. de Jong (✉) · C. Kamenik · M. Grosjean
Institute of Geography, University of Bern, Erlachstrasse 9a, 3012 Bern, Switzerland
e-mail: dejong@giub.unibe.ch

R. de Jong · C. Kamenik · M. Grosjean
Oeschger Centre for Climate Change Research, University of Bern, Zähringerstrasse 25, 3012 Bern, Switzerland

K. Westover
Department of Ecology and Environmental Science, Umeå University, 901 87 Umeå, Sweden

Introduction

Cold-season temperatures in high-elevation areas are relatively poorly reflected in most currently available climate reconstructions and instrumentally measured time series (IPCC 2007). As a result, knowledge of

climatic forcing factors and natural temperature variability in high-Alpine settings during the cold season is limited. In a comparison of central European seasonal temperatures over the past 500 years, Xoplaki et al. (2005) noted a substantial difference in past seasonal temperatures and the occurrence of extremes, with decadal to multi-decadal spring temperature variability nearly double that of autumn temperature variability. Moreover, Beniston (2005) showed that at a Swiss high-Alpine station (Säntis, 2,502 m a.s.l.), positive temperature extremes in the winter season currently exceed those of all other seasons. As highlighted by Diaz et al. (2003), high-mountain environments are very sensitive to climate changes. It is debatable, however, whether the recent rate and amplitude of temperature change at high altitudes during the winter season exceeds changes at low altitudes (Beniston 2005), or whether they are comparable or even lower than in lowland areas, as suggested by Auer et al. (2007) and Kirchner et al. (2013).

Currently, little is known about past annual- to decadal-scale temperature fluctuations in high-Alpine regions, because most meteorological data and reconstructions based on documentary data are from lowland areas. For example, in Switzerland, out of twelve currently homogenized meteorological time series that start in AD 1864, only three come from above 1,500 m a.s.l. (Begert et al. 2005). Auer et al. (2007) reconstructed Alpine temperatures dating back to AD 1750 based on early instrumental records, but the reconstruction of temperatures above 1,500 m was only possible back to AD 1820 because of a lack of high-elevation station data prior to that time (www.zamg.ac.at/histalp/). Pfister (1993) provided monthly-resolved index data for Switzerland since AD 1523, using historical and documentary data. These inferences, however, were also primarily based on data from lowland regions, and although they represent temperature fluctuations at very high precision at the annual time scale, interpretation of decadal to multi-decadal trends in such data is debated (Zorita et al. 2010). In a temperature reconstruction of the greater Alpine area back to AD 1500 (Casty et al. 2005), only five of 98 time series were derived from above 1,500 m, with AD 1820 the earliest starting date for a high-elevation site. Whereas a great number of high-resolution temperature reconstructions based on natural proxies are available for the Alpine region (Trachsel et al. 2012), these primarily represent summer temperatures. Thus, there is a lack of information on past decadal to multi-decadal fluctuations of cold-season temperatures in the high-Alpine region.

This study presents a high-resolution (5-year), quantitative reconstruction of cold-season (Oct–May) temperatures in high-Alpine Lake Silvaplana, situated at 1,789 m a.s.l., in the SE Swiss Alps (Fig. 1). Lake Silvaplana has annually laminated sediments, allowing for (near-) annual analyses and high chronological precision (Blass et al. 2007a; Trachsel et al. 2010). The current reconstruction was based on analysis of chrysophyte stomatocysts, or simply 'cysts' (resting stages produced by the golden-brown algae) that were shown to be reliable indicators of past cold-season temperatures (de Jong and Kamenik 2011; Kamenik and Schmidt 2005; Pla and Catalan 2005, 2011). The transfer function (TF) developed for the Austrian Alps (Kamenik and Schmidt 2005) was adapted for this study and used to reconstruct the 'day of spring mixing' (S_{mix}), which was the most important environmental variable influencing cyst assemblages in this training set. S_{mix} is a climatically meaningful variable because it is significantly correlated to winter-spring temperatures (de Jong and Kamenik 2011; Kamenik and Schmidt 2005).

Thus, we first reconstructed S_{mix} based on the TF approach for the entire study period. We then applied 'calibration in time' (CIT, Von Gunten et al. 2012) for the period AD 1880–2003 to convert S_{mix} (unit: Julian Days) into absolute mean October–May temperatures (in °C) (de Jong and Kamenik 2011). In the present reconstruction, focus is on mean Oct–May temperature variability since AD 1500. This combination of months fulfilled an essential criterion and is ecologically meaningful because chrysophytes are thought to respond to the length of the ice-covered period and/or the timing of ice break-up and subsequent spring mixing (de Jong and Kamenik 2011). At Lake Silvaplana, freezing temperatures begin in mid-October, and ice-on, as recorded in documentary data (AD 1865–1943), occurs in mid-December. Ice break-up takes place on average on 19 May (Livingstone 2009). Thus, the actual 'cold season' in this high-altitude lake lasts from the middle of October–May. Second, this was the time period that persistently yielded the highest r values ($r = -0.58, p_{adj} < 0.001$)(de Jong and Kamenik 2011).

The study site and methods were selected to optimize the criteria formulated by Von Gunten

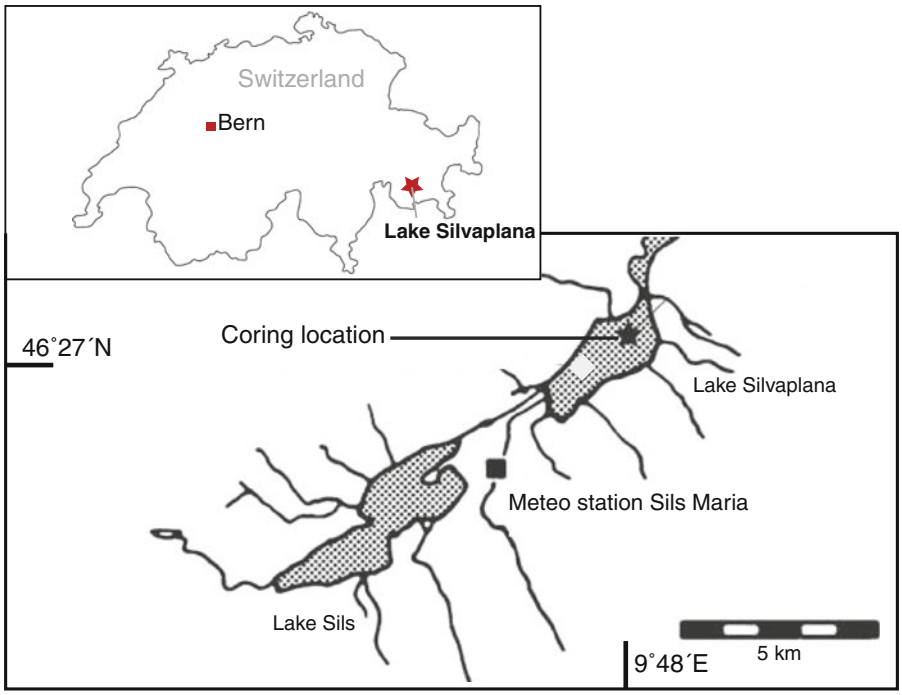

Fig. 1 Overview map of Switzerland and the location of Lake Silvaplana (*inset*) and the study area itself. The coring location and site of the meteorological station Sils Maria are also shown

et al. (2012) for CIT. A much-debated, very important basic assumption in this approach (as in all proxy-based reconstructions) is the notion of stationarity, i.e. the assumption that environmental variables other than S_{mix} (so-called confounding factors; Juggins 2013) have negligible influence on cyst assemblages, or their joint distribution with S_{mix} does not change with time (Juggins 2013; Von Gunten et al. 2012). This issue is highly relevant because most training sets, including the one used here, are designed to cover a long environmental gradient, in this case an altitudinal gradient. Because many environmental variables (e.g. pH, temperature, nutrient concentrations, etc.) change with altitude, TF results may be unrealistic with respect to their ability to reconstruct a single environmental variable reliably (Juggins 2013). The criteria for an optimized reconstruction using TF and CIT apply to this study (Von Gunten et al. 2012) and include: (1) a high-quality, long meteorological time series, (2) a good understanding of lake and catchment processes and undisturbed sedimentation, (3) a precise core chronology, (4) continuous analyses at high resolution, and (5) rigorous testing of the calibration and a good understanding of the relation between the proxy and reconstructed environmental variable. In this study, the quality of the calibration model and reconstruction were tested thoroughly. The assumption of stationarity, which underlies the TF and CIT approaches in this study, is discussed. The climatic implications of this local to sub-regional, high-Alpine study are then placed in a broader context.

Study area

Lake Silvaplana is situated at an altitude of 1,791 m a.s.l. in the Engadine Valley, SE Switzerland (Fig. 1). The Engadine Valley is an inner-Alpine dry valley, characterized by large diurnal and annual temperature ranges, with mean (AD 1961–1990) monthly maximum temperatures occurring in July (10.5 °C) and minimum temperatures in January (−7.3 °C). Data come from the Sils Maria meteorological station, 1,789 m a.s.l. The precipitation maximum (121 mm) occurs in August, whereas minimum precipitation is measured in February (42 mm) (http://www.meteoswiss.admin.ch). Cloud cover at Sils Maria is lowest between October and March, comparable to data from other nearby high-altitude stations

(Säntis, [2,502 m a.s.l.], Davos [1,594 m a.s.l.] and San Bernardino [1,639 m a.s.l.]). Comparison of the relative amount of sunshine measured at low and high altitudes shows that during autumn and winter (Oct–Mar), there is a marked difference, with high altitudes receiving up to 45 % more sunlight. This difference can be explained by the frequent occurrence of high fog at about 800–1,100 m a.s.l., occurring particularly in the northern valleys and lowland areas during autumn and winter, causing the development of an inversion layer, and thus a temporary decoupling of lowland areas from free atmospheric conditions (Auer et al. 2007; Beniston et al. 1997).

Lake Silvaplana is a large (2.7 km^2), deep (77 m) lake of glacio-tectonic origin, with a total volume of 127×10^6 m^3. It is surrounded by mountain peaks reaching 4,000 m a.s.l., with a catchment of 129 km^2, including $\sim$6 km^2 of glaciated terrain (5 % of the catchment area in AD 1998) (Blass et al. 2007b). Sediments from Lake Silvaplana are strongly minerogenic (organic carbon <3 %) and are predominantly composed of silt-size particles. Sediments show annual laminations (varves) from *ca.* 3,300 years ago to present. Varve formation, however, was interrupted briefly from AD 1955 to 1977, likely as a consequence of strong lake eutrophication (Blass et al. 2007a).

Materials and methods

Sediments and core chronology

Cores were collected from the deepest part of the eastern basin, in 77 m of water, using a freeze corer. They extend back to AD 1607 and were complemented by additional piston cores collected in winter 2005/2006. A detailed description of the core sedimentology is provided in Blass et al. (2007b). Annual layers were scraped off the frozen sediment, layer-by-layer, and freeze-dried (Blass et al. 2007b). For cyst analysis, sample treatment followed de Jong and Kamenik (2011). Stomatocyst analysis was carried out using a Zeiss EVO 40 scanning electron microscope. Total cyst and diatom fluxes were reconstructed from a separate set of 0.5-cm-thick subsamples of the same cores, following Bigler et al. (2007). Diatom analysis, cyst:diatom (C:D) ratios and total cyst flux analyses were carried out using a light microscope. To calculate cyst concentrations (cysts cm^{-3} or g^{-1} dry sediment) and accumulation rates (cysts cm^{-2} $year^{-1}$), a known quantity of microspheres was added to the samples, following standard diatom-processing methods (Battarbee and Kneen 1982; Battarbee 1986; Renberg 1990). The updated core chronology (Trachsel et al. 2010) was based on varve counting, corroborated by the AD 1963 and 1986 ^{137}Cs peaks. In addition, turbidite layers were assigned to known historical flood events (Trachsel et al. 2010). The resulting age uncertainty was <4 years for the period since AD 1870 (Kamenik et al. 2010; Trachsel et al. 2010) and was estimated to be 5–10 years between AD 1500 and 1870.

Reconstruction of 'cold-season' temperatures

Chrysophyte stomatocysts were classified following Baumann et al. (2010), Kamenik et al. (2010) and de Jong and Kamenik (2011). Prior to statistical analyses, unornamented cyst types without a collar were combined into only two groups for each size range (small, medium or large); all types with a regular, concave or conical pore, and types with a planar pseudoannulus. This was necessary because of the variable preservation of cysts, which meant these types could not be distinguished with certainty throughout the core.

The number of counted specimens per annual sample was >200 for the period AD 1940–2003, >70 for AD 1870–1940, and >50 for the reconstruction back to AD 1500. To ensure a sufficient total cyst count per sample and reduce the influence of dating errors in the comparison to meteorological data (Koinig et al. 2002), 5-year running sums were calculated prior to further analysis (de Jong and Kamenik 2011). This yielded a final total cyst count per 5-year midpoint of 700 specimens (average, range 350–1,100 specimens) for the calibration period, and 225 specimens (average, range 100–400) for the reconstruction period. Thus, cyst-based S_{mix} and $T_{Oct–May}$ were calculated based on an average specimen count of >225.

Cyst assemblages, including cyst types that exceeded ≥2.5 % and occurred in >6 midpoints, were used to infer dates of spring mixing by applying the TF developed by Kamenik and Schmidt (2005). Lake Silvaplana is in the same altitudinal, and hence temperature range, as the lakes in that training set. Lake Silvaplana, however, is rather large and deep in

comparison, and because of strong lake eutrophication after AD 1952, there are clear differences in water chemistry. Following de Jong and Kamenik (2011), large (>8.8 μm), unornamented cysts and cyst ST151 were excluded from the reconstruction because they were shown to be influenced primarily by nutrient input. Finally, thirteen cyst types were used for the reconstruction of S_{mix}. de Jong and Kamenik (2011) showed that at Lake Silvaplana, dates of spring mixing (S_{mix}) were most strongly correlated to mean October to May air temperatures ($T_{Oct–May}$).

To ensure consistency between the calibration period (post-AD 1864) and the reconstruction period, despite the different number of specimens counted, all calculations for model performance during the calibration period were developed for the entire dataset as well as for a subsampled dataset during the calibration period (Table 1). Thus, from each annual sample during the calibration period, a random subset of 50 specimens was selected. This was repeated 999 times and subsequently, 5-year midpoints were re-calculated, yielding a specimen count of 250. To convert cyst-inferred dates of spring mixing to mean October to May air temperatures, two approaches were tested: (1) inverse regression based on Ordinary Least Squares (OLS) and (2) inverse prediction based on Generalized Least Squares (GLS) (Fox and Weisberg 2010; Venables and Ripley 2002).

Inverse regression is the standard approach when calibrating in time (Trachsel et al. 2010). It assumes that $T_{Oct–May}$ depends on S_{mix}, that only $T_{Oct–May}$ (but not S_{mix}) is associated with errors, and that these errors are uncorrelated. Clearly, these assumptions are not met, as the cyst-based S_{mix} transfer function has a Root Mean Square Error of Prediction (RMSEP) of 7.1 days, and a preliminary Durbin-Watson test revealed that regression residuals were not independent from each other. The GLS approach, in contrast, takes into account that residuals are correlated. Furthermore, inverse prediction assumes that S_{mix} depends on $T_{Oct–May}$, and that S_{mix} (and not $T_{Oct–May}$) is associated with errors. Preliminary autocorrelation and partial autocorrelation functions suggested a moving average (MA) correlation structure of up to order five. For a formal assessment of the order of the underlying MA process, a bias-corrected form of Akaike's information criterion (AIC, Brockwell and Davis 2003) was used. The individual GLS models with MA orders 0–5 (parameter estimation by maximum likelihood) were checked for invertibility, and the (expected) randomness of residuals was checked by the Ljung-Box and McLeod-Li portmanteau tests, the turning point test, the difference-sign test, by fitting an autoregressive model and by checking for normality (Brockwell and Davis 2003). Different GLS models were compared by Analysis of Variance (Fox and Weisberg 2010).

Errors of the different regression approaches were assessed by h-block cross-validation (block size: 4 years), which takes into account serial autocorrelation (Burman et al. 1994).

Ordination of cyst assemblages

An ordination was carried out on the entire cyst assemblage dataset, including all 31 cyst types shown in Fig. 2. The first ordination axis represents the maximum variance in the dataset, which is assumed to represent the most important environmental driver, or a complex interaction of a number of variables that influence the cyst assemblages. Because the TF approach in this study is based on the assumption that S_{mix} is the single environmental parameter driving cyst assemblages, these two curves should look very similar. If this is not the case, then the assumption of stationarity does not hold, and confounding factors (Juggins 2013) may have been, at least temporarily, more important than the variable of interest. The cyst assemblage data were square-root-transformed prior to analysis to reduce the influence of dominant cyst types. To obtain the gradient length of the dataset, a Detrended Correspondance Analysis (DCA) was done, resulting in a gradient length of 1.96 standard deviations. Therefore, Principal Component Analysis (PCA) was carried out because it assumes a linear response of species to the environmental variable of interest. The number of significant PCA axes was tested by comparison to the broken stick model (Jackson 1993).

Calculations were carried out in R (R Development Core Team 2011) with the add-on packages AICcmodavg (Mazerolle 2011), ANALOGUE (Simpson and Oksanen 2009), CAR (Fox and Weisberg 2010), NLME (Pinheiro et al. 2011), RIOJA (Juggins 2009) and VEGAN (Oksanen et al. 2011). Results of time-series analysis were also calculated with the computer program ITSM2000 (Brockwell and Davis 2003).

Table 1 Summary of the OLS and GLS (with the order of the moving average (MA) term given in brackets) regression models tested to convert cyst-inferred date of spring mixing (S_{mix}) into mean $T_{Oct–May}$ (in decreasing order of parsimony)

Models	Coefficients	AIC	Random residuals (Tests passed)	RMSEP (°C)	IQRrecon to IQRmeasured
Inverse regression					
OLS	T = 9.69–0.08 Smix	–	2/6 * (2/6 *)	0.4 (0.4)	0.9 (1.0)
Inverse prediction					
OLS	Smix = 145.6–5.4 T	680 (676)	3/6 (3/6)	0.6 (0.6)	2.0 (2.3)
GLS (1) *	Smix = 147.8–4.5 T Wt = Zt + 0.7 Zt−1	586 (592)	2/6 * (3/6)	0.8 (0.7)	2.4 (2.7)
GLS (2) *	Smix = 149.9–3.57 T Wt = Zt + 1.1 Zt−1 + 0.5 Zt2	534 (561)	2/6 * (1/6 *)	1.0 (0.9)	3.1 (3.4)
GLS (3) *	Smix = 153.2–2.1 T Wt = Zt + 1.2 Zt−1 + 0.9 Zt2 + 0.3 Zt−3	518 (558)	2/6 * (2/6 *)	1.9 (1.3)	5.1 (4.3)
GLS (4) *	Smix = 154.1–1.7 T Wt = Zt + 1.3 Zt−1 + 1.2 Zt2 + 0.9 Zt−3 + 0.5 Zt−4	484 (533)	1/6 * (2/6 *)	2.5 (1.1)	6.5 (4.4)
GLS (5)	Smix = 154.8–1.4 T Wt = Zt + 1.3 Zt−1 + 1.2 Zt2 + 1.0 Zt−3 + 0.6 Zt−4 + 0.1 Zt−5	485 (534)	1/6 * (2/6 *)	No conv. (1.9)	No conv. (5.8)

The second column provides model coefficients as well as the MA parameters, describing the autoregressive time series model for the residuals in GLS models (Brockwell and Davis 2003). Asterisks either denote GLS models that significantly differ from the previous OLS or GLS model (see Models), or significant trends in the residuals (see Random residuals). All model coefficients are significant ($p < 0.05$). Numbers in parentheses present test statistics for models developed on a subset of stomatocysts randomly drawn from the calibration period (post-AD 1864) to mimic cyst analysis for the reconstruction period (pre-AD 1864; see main text). Models were based on 102 (OLS) or 118 (GLS) midpoints, because OLS does not require interpolated data

AIC is a measure of the relative goodness of fit (the lower the better). Information on 'random residuals' summarises test results on the dependence of residuals (if residuals were independent—as assumed by the model—six out of six tests should be passed). RMSEP denotes the error of the model during the calibration period. The ratio of reconstructed versus measured Interquartile Ranges (IQR) indicates whether models deflate or inflate the amplitude of reconstructed temperature (ratio <1 or >1, respectively). No conv. = model did not converge during cross validation

Results

Cyst stratigraphy and reconstructed S_{mix}

Figure 2 shows the 31 most common cyst types that occur in the sediments of Lake Silvaplana since AD 1500. Images of these types can be found on the internet (Kamenik 2010; www.stomatocysts.unibe.ch). Cysts included in the training set and used for the calculation of S_{mix} are indicated in bold. Although the assemblage is dominated by ST157, most likely produced by *Dinobryon* sp., and unornamented cyst types without a collar (medium), the figure shows that other types used for the reconstruction of S_{mix} also occurred regularly and at varying frequencies. After AD 1950, a large number of new cyst types occurred at increased frequencies. As discussed in de Jong and Kamenik (2011), this was related to a marked increase in nutrient loading to the lake, leading to eutrophication. The total abundance of cyst types included in the reconstruction prior to the calibration period was very high (75–92 %). After AD 1950, the abundance of cyst types included in the reconstruction varied from 42 to 70 %.

Reconstructed S_{mix} since AD 1500 is shown in Fig. 3e. S_{mix} varied substantially between 144 and 168 Julian days, which corresponds to dates between 22 May and 16 June. The reconstruction shows that the amplitude of S_{mix} variability (5-year averages) was high throughout the entire period, and that the range of S_{mix} values during the calibration period was as large as the range reconstructed during the preceding period. Bootstrapped sample-specific errors of S_{mix} were highest during the calibration period (range 9.3–14.3 Julian days), when S_{mix} occurred early. Amplitudes of S_{mix} thus exceeded the bootstrapped sample-specific standard errors of prediction (SEP), showing that reconstructed variability was larger than the reconstruction error, but not larger than the corresponding 95 % confidence interval (1.96 * SEP).

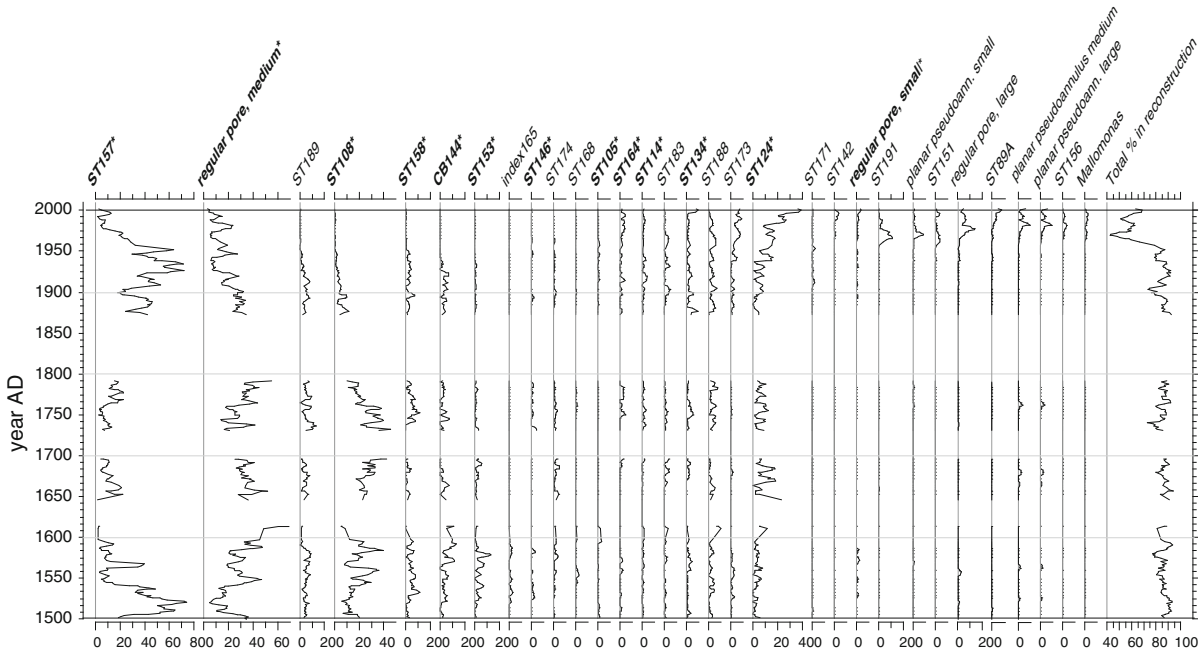

Fig. 2 Stomatocyst stratigraphy, showing percentages of the 31 most common cyst types in the sediments of Lake Silvaplana. *Bold*, marked types were included in the training set and used for the reconstruction of S_{mix}. As a simple indicator for the reliability of the reconstruction, the total % of stomatocyst types that were included in the reconstruction is shown to the right

During three intervals, very few or no cysts could be found (AD 1596–1652, AD 1698–1730, and AD 1795–1873; grey shaded bands in Fig. 3). During these intervals the minerogenic content of the varves was so high that it was impossible to detect sufficient cysts. Figure 3d shows that these periods were characterized by very low reconstructed cyst fluxes and coincided with high mass accumulation rates in Lake Silvaplana (Fig. 3a), large glaciers in the Alpine region (Fig. 3b), and increased cyst:diatom ratios (Fig. 3c).

Cold-season temperature reconstruction and associated errors

Table 1 summarizes the regression models that were tested for converting cyst-based S_{mix} reconstructions into 'cold-season' (mean October–May) temperatures. Autocorrelation functions suggested uncorrelated residuals at lags >3 for both inverse regression and inverse prediction; errors are reported from h-block cross-validation, omitting 4 years on both sides of each individual validation. Inverse OLS regression resulted in the lowest errors (0.4 °C). Because none of the tested models was able to fully meet all theoretical assumptions required for unbiased parameter estimation (Table 1), we used the most parsimonious model that met most theoretical statistical assumptions and resulted in a low RMSEP (inverse OLS regression). Because this model reduced temperature variations (Table 1; IQR_{recon}:$IQR_{measured}$ = 0.9), reconstructed $T_{Oct–May}$ was re-scaled to equal the variance of measured $T_{Oct–May}$ temperatures during the calibration period. The re-scaled error of this reconstruction (root of the re-scaled mean square error of prediction as assessed by h-block cross-validation) was 0.5 °C. This error is, in the strict sense, only valid for the calibration period, but in the CIT approach this is the error commonly used for the entire reconstruction.

Reconstructed cold-season temperatures (5-year averages, Fig. 4c) varied substantially since AD 1500, ranging between −0.7 and −3.6 °C. Maximum values were recorded around AD 1583 (−0.8 °C), AD 1743–1758 (−0.8 °C) and after AD 1980 (−0.7 °C). Minimum reconstructed temperatures occurred around AD 1515 and AD 1885 (−3.6 °C).

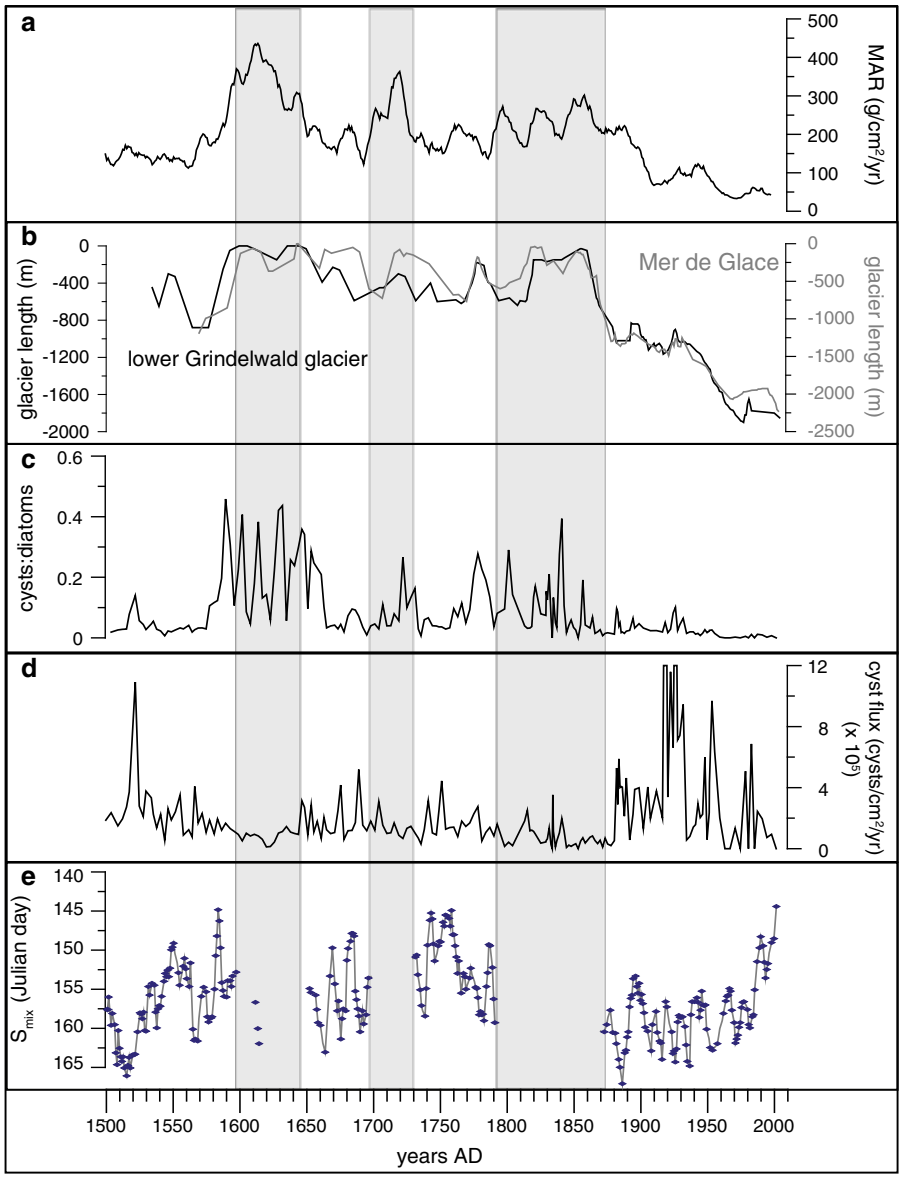

Fig. 3 **a** Mass accumulation rates of sediments in Lake Silvaplana (same material as used in this study) (Trachsel et al. 2010), **b** Lower Grindelwald and Mer de Glace glacier length reconstruction (Nussbaumer et al. 2011; Zumbühl et al. 1983), **c** cyst:diatom ratio, **d** total cyst flux to the sediments of Lake Silvaplana, **e** cyst-based reconstructed S_{mix} (this study). *Diamonds* show actual midpoints based on five consecutive annual samples, the line shows the linear interpolation between these midpoints

Ordination of cyst assemblage data

PCA carried out on the full reconstruction period (AD 1500–2003) yielded a single significant PCA axis that only showed a change around AD 1950. Because the eutrophication change at that time is well known and was not of primary interest to this study, the ordination was repeated for the period AD 1500–1950. For this time frame, comparison to the broken stick model suggested that only the first two PCA axes were significant. The first axis (PCA1) explained 21 % of the variance in the square-root-transformed cyst-assemblage dataset (PCA2 explained 13 %). Figure 5 shows that the pattern of PCA1 is highly comparable

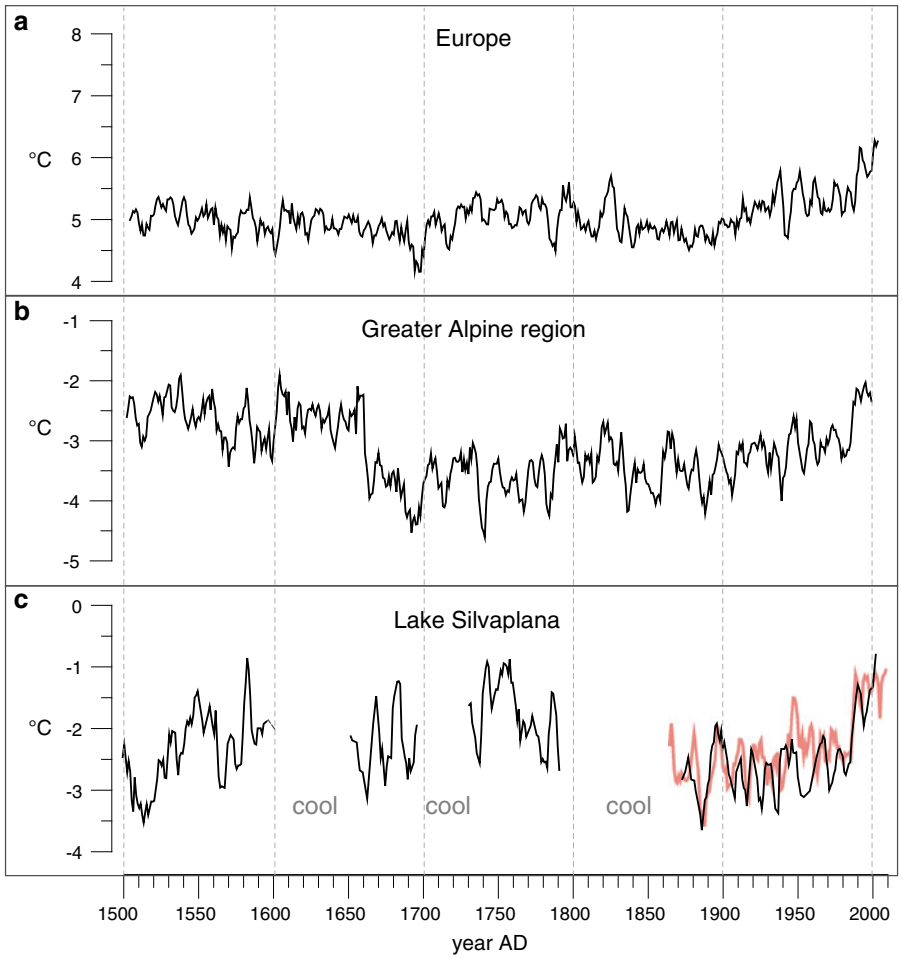

Fig. 4 **a** 'European' Sept-May temperature reconstruction (Luterbacher et al. 2004), **b** 'greater Alpine' Sept-May temperature reconstruction, showing the extracted data for the grid cell including Lake Silvaplana, and **c** Lake Silvaplana October-May temperature reconstruction (this study). Five-year filtered Oct-May temperature data from the nearby meteorological station Sils Maria are shown for the calibration period. To facilitate comparison, the 'European' and 'greater Alpine' records were 5-year filtered

to reconstructed S_{mix}. Because both PCA1 and S_{mix} were based on (part of) the same basic dataset, they are not independent and therefore correlation coefficients and p-values could not be calculated meaningfully.

Discussion

Quality of the reconstruction; basic assumptions

The Silvaplana study area was selected because it optimizes the requirements for quantitative reconstruction of environmental variables. Homogenized, monthly-resolved meteorological data were available from a station near the lake back to AD 1864 (Begert et al. 2005). The presence of annual sediment layers indicates that deposits were undisturbed and the chronology was highly accurate. Continuous analyses were carried out at high resolution whenever possible. The calibration models were tested in detail, as discussed below, but first we address the basic assumption of stationarity.

The most important basic assumption in this proxy-based reconstruction is that the statistical relationships between cyst assemblages, S_{mix} and Oct–May temperatures for the calibration period prevailed back to AD 1500. To test whether this was the case, one has to assess (1) whether major environmental changes, other than cold-season temperature changes,

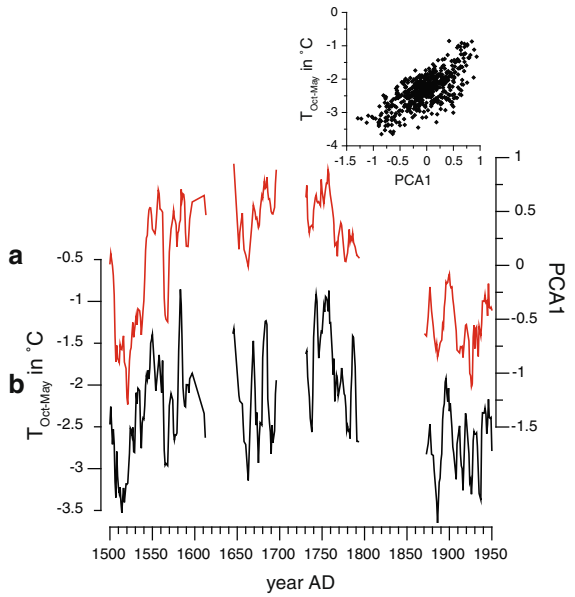

Fig. 5 **a** First PCA axis of the chrysophyte stomatocyst dataset, which was based on the square-root-transformed frequencies of 31 cyst types. The first PCA axis explains 21 % of the total variance in the dataset. **b** Reconstructed Oct–May mean temperatures from AD 1500 to 1950, based on the combined TF and CIT approach. Thirteen cyst types were used for this reconstruction. The inset shows the scatterplot of cold-season temperatures versus PCA1; because both reconstructions derive from the same dataset, however, correlation coefficients and significance levels cannot be assessed meaningfully

influenced the study area, as these have the potential to alter the proxy-environmental variable relation, and (2) assess whether these changes influenced the proxy record to such an extent that the reconstructed climate variable was no longer faithfully recorded in the proxy record.

A multi-proxy approach was required to address these issues. A suite of biological, geochemical and sedimentological properties was reported for Lake Silvaplana in previous studies: varve thickness and mass accumulation rates (Blass et al. 2007b; Trachsel et al. 2010), total biogenic silica fluxes (Blass et al. 2007a; Trachsel et al. 2010), mineral composition (Trachsel et al. 2008), diatom composition (Bigler et al. 2007; Westover, unpublished data) and chironomid assemblages (Larocque et al. 2012). These records show that for the past 500 years, the single most important environmental change was the strong eutrophication after AD 1950. Cyst assemblages also changed substantially after that time (Fig. 2). Thus, the calibration period includes the time period with the strongest environmental disturbance since AD 1500, the lowest analogy to cysts in the training set, and includes samples that have among the highest sample-specific errors (SEP). Despite this weak analogy, reconstructed S_{mix} was significantly correlated to cold-season temperatures throughout the calibration period.

A different approach to see whether environmental changes other than the variable of interest ('confounding variables'; Juggins 2013) influenced cyst assemblages was to compare S_{mix} to the first ordination axis of the full cyst dataset. Because ordination summarizes the maximum variance in the dataset, which is commonly interpreted as reflecting the most important 'external driver or combination of drivers' of changes in large datasets, and the transfer function approach assumes that a given proxy responds to a single, most important environmental variable, in theory reconstructions of S_{mix} and PCA1 should look similar. Figure 5 shows that for the period AD 1500–1950, this was indeed the case. This suggests either that only a single environmental variable primarily controlled cyst assemblages ($T_{Oct–May}$ through S_{mix}) or that the correlation between S_{mix} and confounding variables remained stable through time.

In summary, the similar patterns of the first ordination axis and the $T_{Oct–May}$ curves point to a continuous environmental driver (or set of drivers) controlling cyst assemblages from AD 1500–1950. Results during the full calibration period (de Jong and Kamenik 2010) indicate that the strongest environmental 'disturbance,' the eutrophication phase, did not significantly affect the cyst-S_{mix}-$T_{Oct–May}$ relationships. Apparently, however, different sub-sets of chrysophyte stomatocyst types can respond simultaneously to two different environmental drivers, in this case $T_{Oct–May}$ and eutrophication. This highlights the importance of a multi-proxy approach and detailed comparison of cyst types to other potential environmental drivers, as was done in Kamenik et al. (2010) for chrysophyte stomatocysts in Lake Silvaplana. This allowed us to remove cyst types that are sensitive to eutrophication prior to further analyses.

Error assessment

Table 1 illustrates that the RMSEP for $T_{Oct–May}$ depends heavily on the statistical model used to convert S_{mix} into $T_{Oct–May}$. Models that disregard any dependence among residuals (OLS) resulted in similar RMSEP no matter

whether the RMSEP was estimated by k-fold cross-validation (de Jong and Kamenik 2011) or h-block cross-validation (this study). In contrast, models that take into account residual autocorrelation (GLS) resulted in an RMSEP that was up to five times higher, part of which can be attributed to large uncertainties in the MA parameter estimates. Because the RMSEP is usually used as a criterion for model selection, it is difficult to assess which is the most adequate regression model outside the calibration period. According to its AIC, GLS was the most appropriate model. Tests on residuals, however, illustrated that GLS modeled the residual structure comparable to the more parsimonious OLS inverse regression model, which was therefore selected.

The conventional error of the TF-derived reconstruction (bootstrapped, sample-specific errors) of spring mixing dates was 9.3–14.3 days, with the largest errors occurring during the last four decades of the reconstruction. However, because the calibration period covers the full range of reconstructed S_{mix} (Fig. 3e), ensuring that no linear extrapolation was required for the reconstruction period, and the calibration period includes the decades with the weakest analogy to the training set, the RMSEP derived from OLS regression (0.5 °C) was considered to be a reliable error estimate for the full reconstruction period.

Error components that propagate into the final $T_{Oct–May}$ reconstruction are related to dating uncertainties, counting errors in both the training set and the sediment record, shifts of individual S_{mix} values over time introduced by summing up cyst counts over 5 years (running sums are time-variant), the statistical models used and the corresponding parameter estimation. The lower number of cysts counted during the reconstruction period had no adverse effect on the RMSEP, as illustrated by Table 1. Thus, the strategy of first analyzing low numbers of specimens from consecutive samples at quasi-annual resolution, followed by statistical amalgamation (preferably by time-invariant methods such as weighted sums) is recommended for high-resolution studies of biological assemblages in annually laminated sediments that might cover millennia.

Temperature variability since AD 1500

The cyst record from Lake Silvaplana was interrupted during three time periods (Fig. 3). These three periods coincide with three maxima in mass accumulation rates recorded in the lake (Nussbaumer et al. 2011; Trachsel et al. 2010) and were characterized by low annual fluxes of diatom frustules and cysts and a strong decrease in the cyst:diatom ratio (Fig. 3c, d). These periods also coincided with advanced frontal positions of the Lower Grindelwald and Mer de Glace glaciers (Nussbaumer et al. 2007, 2011; Zumbühl et al. 1983). The high minerogenic influx into the lake was therefore most likely caused by advances of local glaciers, comparable in timing to the glacier advances shown in Fig. 3b. The low biological productivity and increase of the C:D ratio may point to overall cooler temperatures (Smol 1985). It is therefore likely that these 'gaps' represent the occurrence of cold conditions. Comparison to other 'cold-season' records shows that the two most recent gaps (AD 1698–1730, AD 1791–1872) partly coincide with cool events in these records, from AD 1830–1860 for the most recent cold phase (Pfister 1993; Casty et al. 2005) (Fig. 4b). The period from AD 1698–1730 coincides with the coolest phase of the well-known Maunder Minimum. In addition, cool periods were reconstructed around AD 1500–1520, 1567–68, 1614, 1663, 1675, 1690 and 1886 (Fig. 4c), keeping in mind a dating uncertainty of 5–10 years prior to AD 1870.

Ideally, any reconstruction should be compared to other local/regional-scale records that represent the same season. A comparison to other 'cold-season' reconstructions is shown in Fig. 4. This comparison, however, is severely hampered by large differences between the few available cold-season records. Back to AD 1525, seasonally- to monthly-resolved temperature reconstructions based on documentary and historical data are available for Switzerland, a 'winter index' (Pfister 1993, not shown). The 'greater Alpine' (Fig. 4b) temperature reconstruction (Casty et al. 2005), including the Alpine regions of south-western France, Austria, southern Germany and northern Italy, was based on 87 early instrumental time series from all of Europe, combined with 11 documentary records. In that dataset, five sites were situated above 1,500 m. The 'European' reconstruction of cold-season temperature by Luterbacher et al. (2004) was based on a combination of (early) instrumental time series, documentary data, and a number of tree-ring and ice-core records. The records in Fig. 4 have some features in common: cool phases around AD 1510–1520, 1570–1580, shortly before AD 1700 and around AD 1880. Another important common feature is the sharp

warming recorded during recent decades. As expected, differences between the reconstructions are substantial. Primarily, the variability in 'European' reconstruction is much smaller prior to AD 1900, which can be attributed to the large spatial scale of the reconstruction. The applied methodology may also dampen the amplitude of the 'European' and 'Greater Alpine' reconstructions, because these were based on multivariate principal component regression, which, according to Riedwyl et al. (2009) can reduce the amplitude. Similarly, decadal to multi-decadal variability is likely only poorly preserved in reconstructions based on documentary data, as discussed by Zorita et al. (2010).

In addition, these records primarily derive from low-altitude data. There may be substantial differences between temperature patterns (trends and variability) between low- and high-altitude sites (Diaz et al. 2003 and references therein; Beniston 2005; Beniston et al. 1997). Several authors (Beniston et al. 1997; Kirchner et al. 2013) point to the frequent occurrence of a winter inversion layer in valley floors and lowland regions, as illustrated in Fig. 1c by the comparison of sunlight hours at high and low altitudes, which leads to a decoupling of low-altitude sites that are situated under a layer of 'high fog,' from the 'free atmosphere conditions' at higher altitudes. In contrast, Auer et al. (2007) found that centennial and decadal temperature trends since AD 1820, in summer as well as winter, were comparable between high- and low-elevation sites. Clearly, additional highly resolved, high-altitude reconstructions of temperature variability are required to address the long-term trends of winter (or cold-season) temperatures in the high-Alpine region.

High decadal to multi-decadal temperature variability in the high-Alpine region

The current record from Lake Silvaplana should, for the previously mentioned reasons, be regarded as a local to sub-regional (high-Alpine) record. In the cold-season temperature reconstruction presented here, the amplitude varied substantially throughout the past 500 years. The recent cold-season temperature increase recorded in Lake Silvaplana, however, only just exceeded that of previous warm periods, for example around AD 1585 and AD 1750–1760. The reconstructed range of change amounts to *ca.* 24 days (S_{mix}) for the full reconstruction. Support for the reconstructed range of variability can be found in the actual ice break-up dates for Lake Silvaplana, which were recorded between AD 1865 and 1943 (Livingstone 1997). During this short time period, 5-year averages of ice break-up dates displayed a range of 12 days, which is very close to the reconstructed range of S_{mix} during the same time period (14 days) for the same lake.

High past decadal to multi-decadal variability, comparable to warming during recent decennia, was also detected until AD 1950 in a high-Alpine (2,347 m a.s.l.) speleothem record from the Austrian Alps (Mangini et al. 2005). Similarly, high multi-decadal variability was recorded in a summer-temperature reconstruction by Larocque-Tobler et al. (2010) based on chironomid remains in Lake Silvaplana, as well as in the non-disturbed sequence of a pollen-based summer-temperature record from the Mauntschas peat bog (1,818 m a.s.l.) in the vicinity of Lake Silvaplana (Van der Knaap et al. 2011). The $\delta^{18}O$ ice-core record from Colle Gnifetti (4,450 m a.s.l.), known to be a climate proxy, also shows strong decadal and multi-decadal variability over the past 500 years (Sigl 2009). The finding of high-amplitude variability, comparable to recent warming in local studies in high-Alpine settings, is highly relevant in the current climate debate. It shows that although an overall warming trend over large parts of the Northern Hemisphere is, in the research community, practically undisputed (IPCC 2007), local-scale, high-Alpine temperature variability over the past 500 years was much higher than the NH or European-scale means, and is therefore highly unpredictable.

Conclusions

This study illustrates the strength of combining the transfer-function approach with a detailed comparison to meteorological data to construct cold-season temperatures back in time, based on chrysophyte-stomatocyst assemblages. The study was designed to optimize the quantitative reconstruction. Cysts included in the TF were screened against other environmental variables to determine whether they should be included for the reconstruction. Application of the TF provided a reconstruction of a climate-sensitive variable, the date of spring mixing expressed

in Julian Days and associated (conventional) error estimates. Subsequent correlation and linear model building with independent, high-quality meteorological data yielded a reconstruction in degrees Celsius for a clearly defined part of the year, which, because it is a climate variable, is of much greater interest than the TF-derived 'date of spring mixing.' Moreover, it allowed for an alternative error assessment for the calibration period. Both TF and calibration in time, however, depend on the assumption of stationarity, thus the cyst-S_{mix}-$T_{Oct–May}$ relations were assumed to be stable over time. A multi-proxy approach, as well as comparison to the first ordination axis of the cyst data, indicated that stationarity can likely be assumed for this reconstruction. The analyses, however, also indicated that subsets of chrysophyte stomatocysts reflected different environmental drivers simultaneously, post-AD 1950. This stresses the importance of a multi-proxy approach and careful testing of sensitivities of individual cyst types to environmental drivers other than the variable of interest.

The direct comparison of S_{mix} during the calibration period with measured mean monthly temperatures showed that at Lake Silvaplana, cysts can be used as a reliable proxy for past cold-season temperatures. Comparison of S_{mix} to the recorded amplitude of ice break-up dates (AD 1865–1943) on the same lake also confirmed that the reconstructed range of S_{mix} is a good approximation of the directly recorded range of ice break-up and associated spring mixing dates. The statistical relation between reconstructed S_{mix} and measured cold-season temperatures was further explored to optimize the model choice and allow for error estimation. The inverse prediction model, based on OLS, was considered most suitable because it is the most parsimonious model and yielded a low RMSEP of 0.5 °C (re-scaled). The statistical analyses also showed that the strategy of first analyzing low numbers of specimens from consecutive samples at quasi-annual resolution, followed by statistical amalgamation (5-year sums), did not result in increased RMSEPs. This approach can thus be recommended for high-resolution climate reconstructions based on biological proxies in annually laminated sediments, for which low numbers of specimens per sample are often strongly limiting for long-term reconstructions.

The cold-season temperature reconstruction from Lake Silvaplana shows that the range of decadal to multi-decadal cold-season temperature variability during the past 500 years was at least as large (nearly 4 °C for 5-year averages) as temperature variability measured during the last century, until 2003. This is in agreement with long temperature reconstructions from other high-Alpine sites, which show comparable past multi-decadal temperature variability for other seasons. The clear differences between past temperature amplitudes recorded in the continental-scale 'European' reconstruction and the local to sub-regional Silvaplana reconstruction show that small-scale temperature variability in high-Alpine settings may strongly exceed large-scale patterns. It is, however, the variability at smaller scales that is most critical for impacts of climate variability and changes. More quantitative temperature reconstructions from high-Alpine settings are therefore required to fully understand past climate variability and climate processes over a range of spatial scales at high altitudes.

Acknowledgments We thank D. Fischer, E. Baumann, P. Dessarzin and S. Hagnauer for laboratory assistance. Two anonymous reviewers provided helpful comments and suggestions that substantially improved the paper. Discussions on statistical testing and assumptions with M. Trachsel and R. Telford were highly appreciated. Project funding was provided by an EU IEF Marie Curie Grant (PIEF-GA-2008-220189) to R. de Jong. This project is part of the EU FP 6 project Millennium (EU FP6 IP SUSTDEV-2004-3.1.4.1 Contract: 017008).

References

Auer I, Böhm R, Jurkovic A et al (2007) HISTALP – Historical instrumental climatological surface time series of the greater Alpine region 1760-2003. Int J Climatol 27:17–46

Battarbee RW (1986) Diatom analysis. In: Berglund BE (ed) Handbook of holocene palaeoecology and palaeohydrology. Wiley, Chichester, pp 527–570

Battarbee RW, Kneen M (1982) The use of electronically counted microspheres in absolute diatom analysis. Limnol Oceanogr 27:184–188

Baumann E, de Jong R, Kamenik C (2010) A description of sedimentary chrysophyte stomatocysts from high-Alpine Lake Silvaplana (Switzerland). Nova Hedwig Beih 136:71–86

Begert M, Schlegel T, Kirchofer W (2005) Homogeneous temperature and precipitation series of Switzerland from 1864 to 2000. Int J Climatol 25:65–80

Beniston M (2005) Warm winter spells in the Swiss Alps: Strong heat waves in a cold season? A study focusing on climate observations at the Saentis high mountain site. Geophys Res Lett 32:L01812. doi:10.1029/2004GL021478

Beniston M, Diaz HF, Bradley RS (1997) Climatic change at high elevation sites: an overview. Clim Change 36:233–251

Bigler C, von Gunten L, Lotter AF, Hausmann S, Blass A, Ohlendorf C, Sturm M (2007) Quantifying human induced eutrophication in Swiss mountain lakes since AD 1800 using diatoms. Holocene 17:1141–1154

Blass A, Bigler C, Grosjean M, Sturm M (2007a) Decadal-scale autumn temperature reconstruction back to AD 1580 inferred from the varved sediments of Lake Silvaplana (southeastern Swiss Alps). Quat Res 68:184–195

Blass A, Grosjean M, Troxler A, Sturm M (2007b) How stable are 20th Century calibration models? A high resolution summer temperature reconstruction for the eastern Swiss Alps back to A.D. 1580 derived from proglacial varved sediments. Holocene 17:51–63

Brockwell PJ, Davis RA (2003) Introduction to time series analysis and forecasting, 2nd edn. Springer, New York

Burman P, Chow E, Nolan D (1994) A cross-validatory method for dependent data. Biometrika 81:351–358

Casty C, Wanner H, Luterbacher J, Esper J, Böhm R (2005) Temperature and precipitation variability in the European Alps since 1500. Int J Climatol 25:1855–1880. doi:10.1002/joc.1216

de Jong R, Kamenik C (2011) Validation of a chrysophyte stomatocyst-based cold season climate reconstruction from high-Alpine Lake Silvaplana, Switzerland. J Quat Sci 26:268–275. doi:10.1002/jqs.1451

Diaz HF, Grosjean M, Graumlich L (2003) Climate variability and change in high elevation regions: past, present and future. Clim Change 59:1–4

Fox J, Weisberg HS (2010) An R companion to applied regression. Sage Publications, Inc., Thousand Oaks

IPCC (2007) Summary for Policymakers. In: Solomon S, Qin D, Manning M, Chen Z, Marquis M, Averyt KB, Tignor M, Miller HL (eds) Climate Change 2007: The Physical Science Basis. Contribution of Working Group I to the Fourth Assessment Report of the Intergovernmental Panel on Climate Change. Cambridge University Press, Cambridge

Jackson DA (1993) Stopping rules in principal components analysis: a comparison of heuristical and statistical approaches. Ecology 74:2204–2214

Juggins S (2009) Rioja: an R package for the analysis of quaternary science data. (http://www.staff.ncl.ac.uk/staff/stephen.juggins/)

Juggins S (2013) Quantitative reconstructions in palaeolimnology: new paradigm or sick science? Quaternary Sci Rev 64:20–32

Kamenik C (2010) Stom@ocysts & Co – web applications to bring the research community together via the Internet. Nova Hedwig Beih 136:311–323

Kamenik C, Schmidt R (2005) Chrysophyte resting stages: a tool for reconstructing winter/spring climate from Alpine lake sediments. Boreas 34:477–489

Kamenik C, Baumann E, de Jong R, Grosjean M (2010) Effects of cold season climate changes versus anthropogenic nutrient inputs on chrysophyte stomatocyst assemblages (AD 1940–2004) in annually laminated sediments of high-Alpine Lake Silvaplana (Switzerland). Nova Hedwig Beih 136:103–115

Kirchner M, Faus-Kessler T, Jakobi G, Leuchner M, Ries L, Scheele H-E, Suppan P (2013) Altitudinal temperature lapse rates in an Alpine valley: trends and the influence of season and weather patterns. Int J Climatol 33:539–555

Koinig KA, Kamenik C, Schmidt R, Agustí-Panareda A, Appleby P, Lami A, Prazakova M, Rose N, Schnell ØA, Tessadril R, Thompson R, Psenner R (2002) Environmental changes in an alpine lake (Gossenköllesee, Austria) over the last two centuries: the influence of air temperature on biological parameters. J Paleolimnol 28:147–160

Larocque-Tobler I, Grosjean M, Heiri O, Trachsel M, Kamenik C (2010) Thousand years of climate change reconstructed from chironomid subfossils preserved in varved lake Silvaplana, Engadine, Switzerland. Quat Sci Rev 29:1940–1949

Livingstone DM (1997) Break-up dates of Alpine lakes as proxy data for local and regional mean surface air temperature. Clim Change 37:407–439

Luterbacher J, Dietrich D, Xoplaki E, Grosjean M, Wanner H (2004) European seasonal and annual temperature variability, trends, and extremes Since 1500. Science 303:1499–1503. doi:10.1126/science.1093877

Mangini A, Spötl C, Verdesa P (2005) Reconstruction of temperature in the Central Alps during the past 2000 yr from a δ18O stalagmite record. Earth Planet Sci Lett 235:741–751

Mazerolle MJ (2011) AICcmodavg: Model selection and multimodel inference based on (Q)AIC(c). http://cran.r-project.org/package=AICcmodavg

Nussbaumer SU, Zumbühl HJ, Steiner D (2007) Fluctuations of the Mer de Glace (Mont Blanc area, France) AD 1500–2050: an interdisciplinary approach using new historical data and neural network simulations. Zeitschrift für Gletscherkunde und Glazialgeologi 40:1–183

Nussbaumer SU, Steinhilber F, Trachsel M, Breitenmoser P, Beer J, Blass A, Grosjean M, Hafner A, Holzhauser H, Wanner H, Zumbühl HJ (2011) Alpine climate during the Holocene: a comparison between records of glaciers, lake sediments and solar activity. J Quat Sci 26:703–713. doi:10.1002/jqs.1495

Oksanen J, Blanchet FG, Kindt R, Legendre P, O'Hara RB, Simpson G, Solymos P, Henry M, Stevens HH, Wagner H (2011) vegan: Community Ecology Package. http://CRAN.R-project.org

Pfister C (1993) Historical Weather Indices from Switzerland. IGBP PAGES/World Data Center-A for Paleoclimatology Data Contribution Series # 93-027. NOAA/NGDC Paleoclimatology Program, Boulder CO, USA

Pinheiro J, Bates D, DebRoy S, Sarkar D, R Core team (2011) nlme: Linear and Nonlinear Mixed Effects Models, http://www.r-project.org

Pla S, Catalan J (2005) Chrysophyte cysts from lake sediments reveal the submillennial winter/spring climate variability in the northwestern Mediterranean region throughout the Holocene. Clim Dyn 24:263–278

Pla S, Catalan J (2011) Deciphering chrysophyte responses to climate seasonality. J Paleolimnol 46:139–150. doi:10.1007/s10933-011-9529-6

R Development Core Team (2011) R: a language and environment for statistical computing. Austria, Vienna

Renberg I (1990) A procedure for preparing large sets of diatom slides from sediment cores. J Paleolimnol 4:87–90

Riedwyl N, Küttel M, Luterbacher J, Wanner H (2009) Comparison of climate field reconstruction techniques: application to Europe. Clim Dyn 32:381–395. doi:10.1007/s00382-008-0395-5

Sigl M (2009) Ice core based reconstruction of past climate conditions from Colle Gnifetti, Swiss Alps, Ph.D. thesis, Paul Scherrer Institute, Univ. of Bern, Switzerland

Simpson GL, Oksanen J (2009) Analogue: analogue matching and modern analogue technique transfer function models. http://cran.r-project.org

Smol JP (1985) The ratio of diatom frustules to chrysophycean statospores: a useful paleolimnological index. Hydrobiologia 123:199–208

Trachsel M, Eggenberger U, Grosjean M, Blass A, Sturm M (2008) Mineralogy-based quantitative precipitation and temperature reconstructions from annually laminated lake sediments (Swiss Alps) since AD 1580. Geophys Res Lett 35:L13707. doi:10.1029/2008GL034121

Trachsel M, Grosjean M, Larocque-Tobler I, Schwikowski M, Blass A, Sturm M (2010) Quantitative summer temperature reconstruction derived from a combined biogenic Si and chironomid record from varved sediments of Lake Silvaplana (south-eastern Swiss Alps) back to AD 1177. Quat Sci Rev 29:2719–2730. doi:10.1016/j.quascirev.2010.06.026

Trachsel M, Kamenik C, Grosjean M, McCarroll D, Moberg A, Brázdil R, Büntgen U, Dobrovolný P, Esper J, Frank DC, Friedrich M, Glaser R, Larocque-Tobler I, Nicolussi K, Riemann D (2012) Multi-archive summer temperature reconstruction for the European Alps, AD 1053-1996. Quat Sci Rev 46:66–79

van der Knaap WO, Lamentowicz M, van Leeuwen JF, Hangartner S, Leuenberger M, Mauquoy D, Goslar T, Mitchell EA, Lamentowicz L, Kamenik C (2011) A multiproxy, high-resolution record of peatland development and its drivers during the last millennium from the subalpine Swiss Alps. Quat Sci Rev 30:3467–3480

Venables WN, Ripley BD (2002) Modern applied statistics with S, 4th edn. Springer, New York

Von Gunten L, Grosjean M, Kamenik C, Fujak M (2012) Urrutia R (2012) Calibrating biogeochemical and physical climate proxies from non-varved lake sediments with meteorological data: methods and case studies. J Paleolimnol 47:583–600. doi:10.1007/s10933-012-9582-9

Xoplaki E, Luterbacher J, Paeth H, Dietrich D, Steiner N, Grosjean M, Wanner H (2005) European spring and autumn temperature variability and change of extremes over the last half millennium. Geophys Res Lett 32:L15713. doi:10.1029/2005GL023424

Zorita E, Moberg A, Leijonhufvud L, Wilson R, Brázdil R, Dobrovolný P, Luterbacher J, Böhm R, Pfister C, Riemann D, Glaser R, Söderberg J, González-Rouco F (2010) European temperature records of the past five centuries based on documentary/instrumental information compared to climate simulations. Clim Change 101:143–168. doi:10.1007/s10584-010-9824-7

Zumbühl HJ, Messerli B, Pfister C (1983) Die Kleine Eiszeit: Gletschergeschichte im Spiegel der Kunst. Katalog zur Sonderausstellung des Schweizerischen Alpinen Museums Bern und des Gletschergarten-Museums Luzern vom 09.06.–14.08.1983 (Luzern), 24.08.–16.10, Bern